Precision Polymers

International Edition: DOI: 10.1002/anie.201902217
German Edition: DOI: 10.1002/ange.201902217

Learning from Peptides to Access Functional Precision Polymer Sequences

Eva Maron, Jordan H. Swisher, Joris J. Haven, Tara Y. Meyer, Tanja Junkers, and Hans G. Börner**

Abstract: *Functional precision polymers based on monodisperse oligo(N-substituted acrylamide)s and oligo(2-substituted-α-hydroxy acid)s have been synthesized. The discrete sequences originate from a direct translation of side-chain functionality sequences of a peptide with well-studied properties. The peptide was previously selected to solubilize the photosensitizer meta-tetra(hydroxyphenyl)chlorin. The resulting peptidomimetic formulation additives preserve the drug solubilization and release characteristics of the parent peptide. In some cases, superior properties are obtained, reaching up to 40 % higher payloads and 27-times faster initial drug release.*

Although nature provides valuable templates for engineering properties by using sequences in biomacromolecules, the transfer of these general principles to nonbiological polymers still remains challenging. Molecular precision in information-rich macromolecules such as RNA/DNA, oligosaccharides, and peptides/proteins is considered to be the key to the origin of highly selective functions in biosystems.[1] Recently, this concept has been extended to precision polymers,[2] including monodisperse macromolecules with discrete sequences from artificial monomer alphabets. This class of polymers broadly expands the chemical space of backbone constituents and side-chain functionalities compared to biomacromolecules. Precision polymers can be prepared using solid-phase synthesis (SPS)[3] and solution-phase strategies. The latter include radical-chain growth of spontaneous sequence-forming monomers, cyclopolymerizations of templated monomer pairs, and ring-opening metathesis of cyclic macromonomers.[4] Moreover, radical polymerization under single unit monomer insertion (SUMI) conditions and segmer assembly polymerization (SAP) have proven particularly valuable for accessing macromolecules with distinct monomer order.[5]

Sequence-defined macromolecules have already found use in information coding for data storage and anti-counterfeiting applications.[6] Moreover, discrete patterns in polarity and functionality proved to be advantageous for antimicrobial properties and self-assembly control.[7] Certainly the structural and sequential spaces of precision polymers offer new opportunities to explore advanced functions that rely on sequence-specific interactions.[8] Despite the progress on both the synthetic and application fronts, the development of methods to guide the sequence design of precision polymers has received little attention.

Peptides represent a model platform with well-investigated sequence-function relationships that enable nanostructures, hierarchically self-assembled materials, drug-specific carriers, and material-specific adhesives to be programmed, for example.[9] Several approaches have emerged for the de novo design of functional peptides: 1) empiric, 2) combinatorial, 3) rational, 4) bio-inspired, and 5) computational design strategies.[10] The first two approaches seem applicable for the design of precision polymers, as the others are challenging due to the lack of established structure–property relationships in nonbiological macromolecules.

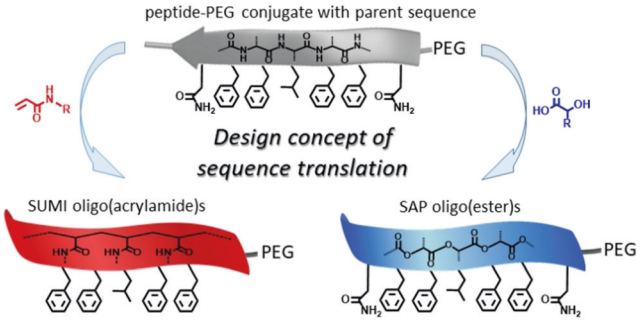

Figure 1. Schematic illustration of the sequence transfer strategy from a peptide-PEG conjugate to PEG-conjugated precision sequences.

Herein, we describe a route for designing functional precision polymers by the translation of peptide sequences into precision polymers by monomer-to-monomer mapping of the peptide side-chain functionalities (Figure 1). A peptide that was previously selected to host *meta*-tetra(hydroxyphenyl)chlorin (*m*-THPC) as a photosensitizer for photodynamic cancer therapy was chosen as a template.[11] Monodisperse *N*-

[*] E. Maron, Prof. H. G. Börner
Department of Chemistry
Humboldt-Universität zu Berlin
Brook-Taylor-Strasse 2, 12489 Berlin (Germany)
E-mail: h.boerner@hu-berlin.de
J. H. Swisher, Prof. T. Y. Meyer
Department of Chemistry
University of Pittsburgh
Pittsburgh, PA (USA)
Dr. J. J. Haven, Prof. T. Junkers
Polymer Reaction Design Group
School of Chemistry, Monash University
19 Rainforest Walk, Clayton VIC 3800 (Australia)
E-mail: Tanja.Junkers@monash.edu
Prof. T. Junkers
Institute for Materials Research, Hasselt University
Martelarenlaan 42, 3500 Hasselt (Belgium)
Supporting information and the ORCID identification number for one of the authors of this article can be found under: https://doi.org/10.1002/anie.201902217.

substituted oligo(acrylamide)s and α-carbon-substituted oligo(ester)s were synthesized by SUMI and SAP procedures. The *m*-THPC loading and release properties of the poly(ethylene glycol) (PEG) conjugated precision sequences were analyzed and compared to the properties of the parent peptide-PEG conjugates.

The peptide-PEG conjugate QFFLFFQ-PEG had previously been shown to be a suitable solubilizer for *m*-THPC, reaching payload capacities of up to 1:3.3 (mol ratio drug/carrier).[11,12] Intriguingly, the peptide sequence indicated a drug-structure-specific hosting of *m*-THPC and thus offers an interesting starting point to explore peptidomimetic precision polymers.[13] The sequence analysis by systematic alanine substitution (Ala scan) indicated the high importance of the FFLFF segment for drug loading, as substitution in this domain dramatically reduced loading.

Exchange of the polar Gln1 or Gln7 residues increased the loading by 14% to 39%.[13] The single residue mutation revealed the importance of Leu4 for drug hosting. The gradual reduction in hydrophobicity by substituting Leu4 in the peptide-PEG conjugate by Val4 and Ala4 reduced the payload by 58% and 92%, respectively (Table S5). This finding is consistent with heme-face contacts in proteins often involving Leu residues for cofactor anchoring.[14]

The effects of the peptide sequence variation on drug release kinetics were studied by a fluorescence-based assay. In *m*-THPC/peptide-PEG complexes the drug is present in a non-active transport state; singlet O_2 production and fluorescence is not measurable, as a result of self-quenching. When BSA (bovine serum albumin) is added, *m*-THPC/BSA complexes are formed and the fluorescence activity is recovered, which can be followed by fluorescence spectroscopy (see the Supporting Information).[11] Although retardation of drug release is of interest for many drug transporters, *m*-THPC solubilization profits from a fast release to blood plasma proteins to rapidly activate the photosensitizer and prevent adverse effects such as extended sensitivity of patients to light.[15] The initial release rates from drug-loaded solubilizers were determined by first-order derivatives of the release traces (Table S5) and suggest the importance of the flanking Gln residues for release. Whereas the lack of Gln1 and Gln7 leads to slow release, single Gln→Ala exchanges result in conjugates that still release with suitable rates. The impact of central residue exchanges (Leu4→Val4→Ala4) on release kinetics is less significant than their effects on loading. For example, QFFAFFQ-PEG shows only a slightly faster release compared to the parent conjugate (Figure S29).

Taking into account the requirements for peptides to reach a high payload and effective release kinetics, precision polymers were designed by direct translation of the side-chain functionality sequences found in the parent peptide. Oligo(*N*-substituted acrylamide)s and oligo(2-substituted-α-hydroxy acid)s were explored as precision polymer platforms.

Monodisperse oligo(acrylamide)s show close chemical similarity to peptides, with the amide functionality preserved, but shifted from the backbone into the side chain, thus establishing a compact C–C backbone. Unsubstituted acrylamide and acrylamides with benzyl, isobutyl, isopropyl, or methyl *N*-substituents define the analogues monomer alphabet to Gln, Phe, Leu, Val, and Ala residues, required to mimic the QFFL(V/A)FFQ peptides. The monodisperse oligomers were prepared by reversible addition-fragmentation chain-transfer polymerization (RAFT) under SUMI conditions (Figure 2 and see the Supporting Information). The chain-transfer agent (CTA) 2-cyano-2-propyl ethyl trithiocarbonate mediated the polymerization of the different acrylamides. The products were purified after each extension step. After completion of the pentamer sequences, the RAFT end groups were aminolysed and the ω-thiol functional penta(acrylamide)s reacted in an in situ Michael addition with acrylamide-ω-functionalized PEG to yield the SUMI-PEG conjugates ($SUMI^{FFLFF}$-PEG, $SUMI^{FFVFF}$-PEG, and $SUMI^{FFAFF}$-PEG).

To decouple the backbone effects from the side-chain sequence, a set of oligo(2-substituted-α-hydroxy acid) segments with analogous side-chain sequences was prepared by SAP procedures (Figure 2 and see the Supporting Information).[8] L-Phenyllactic acid, L-hydroxyisocaproic acid, L-hydroxyisovaleric acid, L-lactic acid, and *N*-(triphenylmethyl)-L-2-hydroxy-4-carbamoylbutanoic acid constituted the monomer alphabet, which corresponds to Phe, Leu, Val, Ala, and Gln. Iterative Steglich esterification, deprotection, and purification steps produced the α-silyl-ω-benzyl-protected hexamers (Figure 2). The final heptamer sequences were accessed by addition of a silyl-protected monomer at the deprotected hydroxy-functionalized α-chain end. Deprotection of the carboxylate ω-chain end allowed coupling of a monomethoxy-substituted PEG. A final deprotection yielded a set of SAP-PEGs that includes $SAP^{QFFLFFQ}$-PEG, the single point-mutated sequences $SAP^{QFFVFFQ}$-PEG and $SAP^{QFFAFFQ}$-PEG, as well as the sequence isomers SAP^{QLFFFQ}-PEG and $SAP^{QFFFLFQ}$-PEG (see the Supporting Information).

In order to investigate analogies to the peptide-PEG conjugates, the oligo(acrylamide)-PEGs and oligo(ester)-PEGs were studied for both their *m*-THPC loading capacities and release properties to BSA. Independent of the sequences, the SUMI-PEGs exhibited slightly lower water solubility than the SAP-PEGs. This difference might be rationalized by stronger interchain interactions of the amide functionalities through the formation of hydrogen bonds in proximity to the hydrophobic C–C backbone. The solubilizers were loaded with *m*-THPC by following a previously established forced-loading procedure.[11] The loading led to a sample set of well-defined *m*-THPC/solubilizer complexes in water. Dynamic light scattering (DLS; Table S4) studies indicated aggregates with hydrodynamic radii (R_H) of 70–78 nm for the drug-loaded SUMI-PEGs, irrespective of the sequence. The loaded SAP-PEGs formed slightly bigger aggregates, with R_H values of 73–85 nm. Hence, all the drug/solubilizer complexes exhibited $R_H < 100$ nm with polydispersities below 0.05 and meet the requirements for biomedical applications.[16]

The $SUMI^{FFLFF}$-PEG solubilizer with the sequence from the parent peptide reached the highest payload capacity of 1:2.3 (mol ratio drug/carrier). This capacity corresponds to an increase of 40% compared to the optimized peptide-PEG conjugate (Figure 3). Interestingly, the capacities of the SUMI-PEG constructs follow the same trend as found in

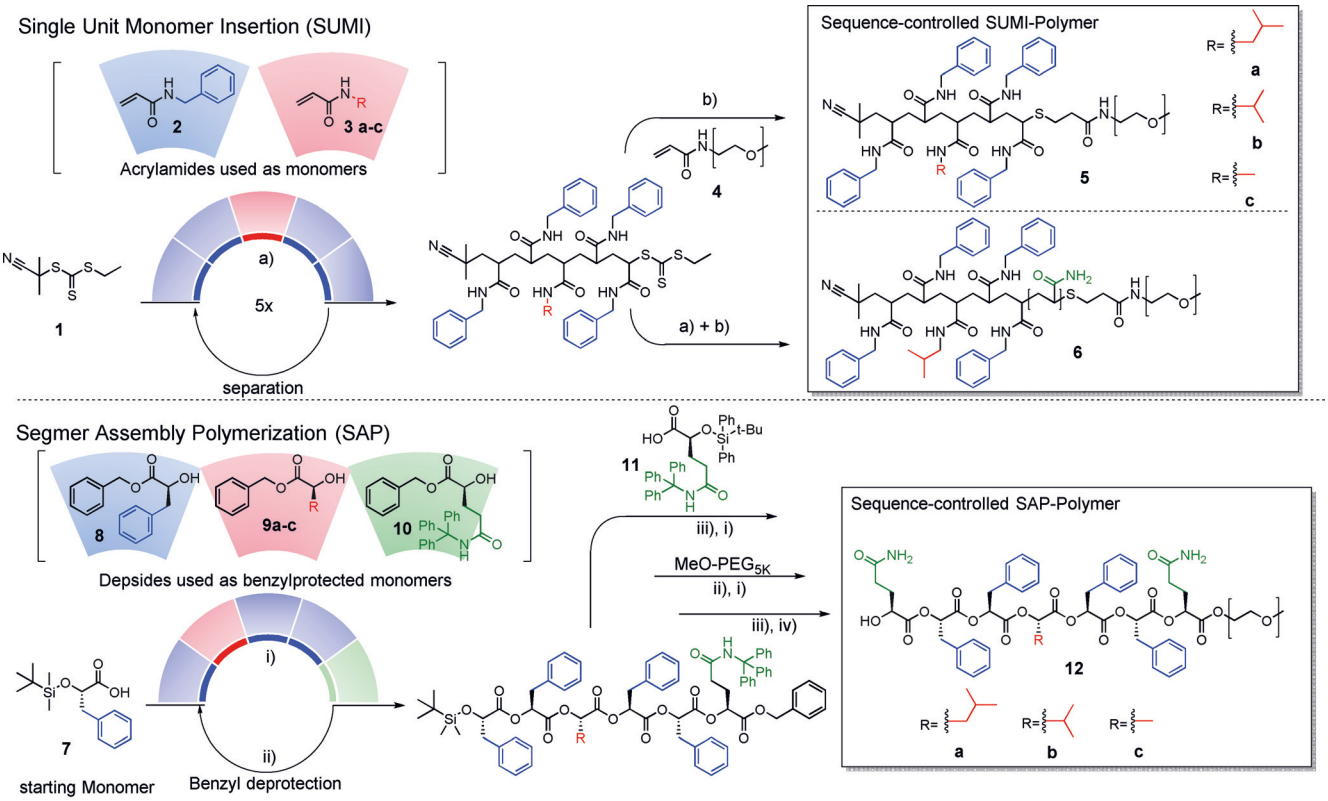

Figure 2. Synthesis of sequence-defined oligomer-PEG conjugates by SUMI to afford oligo(acrylamide)-PEGs (top), and by SAP to give poly(ester)-PEGs (bottom). Conditions: a) AIBN/CTA in dioxane/water; b) hexylamine/tributylphosphine, $CHCl_3$; i) DCC/DPTS, DCM; ii) Pd/C, H_2; iii) TBAF/AcOH, THF; iv) TFA/DCM. AIBN = 2,2′-azobisisobutyronitrile, DCC = dicyclohexylcarbodiimide, DCM = dichloromethane, DPTS = 1,4-dimethylpyridinium *p*-toluenesulfonate, TBAF = tetrabutylammonium fluoride.

the peptide-PEG conjugates with systematic substitution of the central residues. The Leu analogue had the highest capacity, while a significant decrease to 1:4.3 and 1:7.6 (mol ratio drug/carrier) was observed on changing the central isobutyl side chain to isopropyl ($SUMI^{FFVFF}$-PEG) and methyl ($SUMI^{FFAFF}$-PEG) (Figure 3). The 60% reduction in the payload capacity in going from $SUMI^{FFLFF}$-PEG to $SUMI^{FFAFF}$-PEG is quite dramatic. The observed sensitivity of the SUMI-PEG solubilizer payload, which exceeds that expected for a decrease in the volume fraction of the hydrophobic segment, suggests specific binding interactions between the drug and SUMI domains.

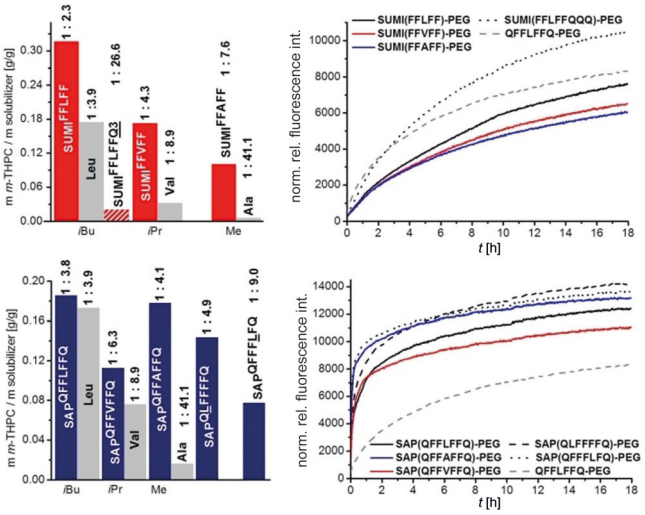

Figure 3. Drug-uptake (left) and release (right) properties of SUMI-PEG (top) and SAP-PEG solubilizers (bottom). Payload capacities were normalized to the functional segment masses and values over the columns correspond to the drug/carrier molar ratio.

The solubilizer $SAP^{QFFLFFQ}$-PEG, with the directly translated peptide sequence, reached a *m*-THPC loading of 1:3.8 (mol ratio drug/carrier). Normalized by the mass of the functional segment, this capacity matches well with that of the parent peptide conjugate (Figure 3). Interestingly, $SAP^{QFFVFFQ}$-PEG and $SAP^{QFFAFFQ}$-PEG bearing isopropyl and methyl substituents exhibited capacities of 1:6.3 (−41%) and 1:4.1 (−11%), respectively. This behavior varies from what was observed with the peptide or SUMI solubilizers. It might be rationalized by the fact that the amide to ester translation reduces the contrast in the hydrophobicity between the backbone and side chains, such that the variation from *i*Bu to *i*Pr to Me has little impact. The sequence, however, appears to play a significant role for these SAP segments. If the central Leu analogue residue is shifted, substantial reductions in the loading capacity of 22% and 59% were observed for $SAP^{QLFFFFQ}$-PEG and $SAP^{QFFFLFQ}$-PEG, respectively. The shift of the central residue destroys the FF-analogous dyads, which will probably disturb π-π interactions with the chlorin structure.

Despite the structural relationship of peptides and oligo(acrylamide)s, all the *m*-THPC/SUMI-PEG complexes show slow release kinetics (Figure 3, see also Table S5). Counterintuitively, the impact of side-chain alteration is evidently less dominant in terms of the release kinetics than on payload capacities in the case of SUMI-PEG solubilizers. Apparently, the side-chain amides of the oligo(acrylamide) provide insufficient polarity to counterbalance the removal of both flanking Gln analogue residues. In this respect, the release properties of the SUMI-PEG conjugates mimic the behavior of the parent peptide-PEG solubilizer, which converts into a slow releaser in the case when Gln1 and Gln7 are removed (Figure S29). Analyzing the peptides showed that a single Gln→Ala exchange is tolerated (regardless of Gln1 or Gln7) and preserve the fast release of the peptide-PEG solubilizers. Therefore, faster release was expected on extending the SUMI^{FFLFF} segment with a small block of acrylamide residues to give SUMI$^{FFLFFQ^3}$-PEG (Figure 3). As predicted, the polar sequence variant resulted in the *m*-THPC/SUMI$^{FFLFFQ^3}$-PEG complexes showing dramatically enhanced release kinetics, superior to the performance of the parent QFFLFFQ-PEG solubilizer (Figure 3). The increased polarity of the SUMI-PEG solubilizer provides sufficient interface activity to assist the *m*-THPC transfer from the hydrophobic core of the drug/solubilizer complexes to BSA in the aqueous phase. The delicate balance in the hydrophilicity/hydrophobicity along the SUMI segments evidently affects the payload capacity. These results highlight the importance of the precision segment, as the effect cannot simply be a consequence of the extension of the polar PEG block.

Interestingly, all the oligo(ester)s show a preferred burst-type of release, which is associated with the molecular structures of the SAP segments, as no hydrolytic degradation was evident during loading and release experiments. The activation of *m*-THPC from SAP-PEG drug complexes is significantly faster than is observed from drug complexes of the parent peptide-PEG conjugate or the SUMI$^{FFLFFQ^3}$-PEG solubilizer (Figure 3). For example, *m*-THPC/SAP^{QFFLFFQ}-PEG complexes activate about 70% of the releasable photosensitizer within 1.5 h, which would be suitable for therapeutic applications. In the set of *m*-THPC/SAP-PEG complexes, the release rates were rather similar, making a solid interpretation difficult. However, both SAP-PEG solubilizers with isosequences show even faster initial drug release rates than the nonscrambled SAP^{QFFLFFQ}-PEG (Figure 3, see also Table S5). The presence of sequence-specific interactions is suggested by the fact that moving the Leu analogue residue by one sequence position to give SAP$^{QFFF\underline{L}F\underline{Q}}$-PEG leads to the fastest initial release rates of the entire set. Probably, the single position change weakens the interactions of the precision segment SAP$^{QFFF\underline{L}F\underline{Q}}$ with *m*-THPC and increases the transfer rates to BSA. The set of oligo(ester)s reveals that trans-solubilization is influenced primarily by the functional sequences. The backbone structure, in turn, appears to exhibit a significant effect on the release, as the backbone contributes to modulation of drug binding interactions, phase-transfer capabilities, and the structural dynamics of the solubilizer segments in drug/solubilizer complexes.

In conclusion, the drug-hosting peptide (QFFLFFQ) that was identified to accommodate *m*-THPC could be directly translated into sequences of precision polymers, with preserved properties of the parent peptide. Two sets of peptidomimetic precision polymers, based on oligo(*N*-substituted acrylamide)s and oligo(2-substituted α-hydroxy acid)s were prepared. The corresponding PEG conjugates mimic properties of the parent peptide-PEG drug solubilizer and show up to 40% higher payloads and the desired drug release profile. The SUMI-PEGs mimic the sensitivity of the payload capacity on single point mutation of the central Leu residue and show the same retardation of release kinetics on removal of the flanking Gln analogues, as found in analogous peptide sequences. The SAP-PEGs show less sensitivity to mutations of central residues, but have a clear sensitivity to the monomer order in terms of the payload and release. The translation strategy might be broadly applicable for materials science applications and guide the design of precision polymers where advanced functions originate from sequence-specific interactions.

Acknowledgements

H.G.B. acknowledges financial support by the European Research Council under the European Union's 7th Framework Program (FP07-13)/ERC Consolidator grant "Specifically Interacting Polymer-SIP" (ERC 305064). T.Y.M. acknowledges financial support from the National Science Foundation (CHE-1709144). Additional support for MALDI-TOF MS instrumentation was provided by a grant from the National Science Foundation (CHE-1625002). T.J. and J.J.H. are grateful for provision of the mass spectrometer through the Hercules fund Belgium. J.J.H. and T.J. thank J. Vandenbergh for contributing to the synthesis of the SUMI oligomers.

Conflict of interest

The authors declare no conflict of interest.

Keywords: drug delivery system · monodisperse polymers · peptide PEG conjugates · precision polymers · sequence design

How to cite: *Angew. Chem. Int. Ed.* **2019**, *58*, 10747–10751
Angew. Chem. **2019**, *131*, 10858–10863

[1] J. M. Berg, J. L. Tymoczko, L. Stryer, W. H. Freeman, *Biochemistry*, 7th ed., Palgrave MacMillan, New York, **2002**.

[2] a) M. Ouchi, N. Badi, J.-F. Lutz, M. Sawamoto, *Nat. Chem.* **2011**, *3*, 917–924; b) H. G. Börner, *Macromol. Rapid Commun.* **2011**, *32*, 115–126; c) J.-F. Lutz, J.-M. Lehn, E. W. Meijer, K. Matyjaszewski, *Nat. Rev. Mater.* **2016**, *1*, 16024.

[3] a) J. M. Stewart, J. D. Young, *Solid-Phase Peptide Synthesis*, 2nd ed., Pierce Chemical Company, Rockford, **1984**; b) S. L. Beaucage, R. P. Iyer, *Tetrahedron* **1992**, *48*, 2223–2311; c) O. J. Plante, E. R. Palmacci, P. H. Seeberger, *Science* **2001**, *291*, 1523–1527; d) J. M. Kerr, S. B. H. Kent, W. H. Moos, R. N. Zuckermann, *J. Am. Chem. Soc.* **1992**, *114*, 10646–10647; e) O. Kuisle, E. Quiñoá, R. Riguera, *J. Org. Chem.* **1999**, *64*, 8063–8075; f) L.

Hartmann, E. Krause, M. Antonietti, H. G. Börner, *Biomacromolecules* **2006**, *7*, 1239 – 1244; g) L. Hartmann, H. G. Börner, *Adv. Mater.* **2009**, *21*, 3425 – 3431; h) A. Al Ouahabi, L. Charles, J.-F. Lutz, *J. Am. Chem. Soc.* **2015**, *137*, 5629 – 5635; i) S. C. Solleder, D. Zengel, K. S. Wetzel, M. A. R. Meier, *Angew. Chem. Int. Ed.* **2016**, *55*, 1204 – 1207; *Angew. Chem.* **2016**, *128*, 1222 – 1225; j) S. Celasun, D. Remmler, T. Schwaar, M. G. Weller, F. Du Prez, H. G. Börner, *Angew. Chem. Int. Ed.* **2019**, *58*, 1960 – 1964; *Angew. Chem.* **2019**, *131*, 1980 – 1984; k) S. Martens, J. Van den Begin, A. Madder, F. E. Du Prez, P. Espeel, *J. Am. Chem. Soc.* **2016**, *138*, 14182 – 14185; l) R. K. Roy, A. Meszynska, C. Laure, L. Charles, C. Verchin, J.-F. Lutz, *Nat. Commun.* **2015**, *6*, 7237; m) D. de Rochambeau, M. Barłóg, T. G. W. Edwardson, J. J. Fakhoury, R. S. Stein, H. S. Bazzi, H. F. Sleiman, *Polym. Chem.* **2016**, *7*, 4998 – 5003.

[4] a) K. Satoh, M. Matsuda, K. Nagai, M. Kamigaito, *J. Am. Chem. Soc.* **2010**, *132*, 10003 – 10005; b) Y. Hibi, S. Tokuoka, T. Terashima, M. Ouchi, M. Sawamoto, *Polym. Chem.* **2011**, *2*, 341 – 347; c) Y. Hibi, M. Ouchi, M. Sawamoto, *Angew. Chem. Int. Ed.* **2011**, *50*, 7434 – 7437; *Angew. Chem.* **2011**, *123*, 7572 – 7575; d) W. R. Gutekunst, C. J. Hawker, *J. Am. Chem. Soc.* **2015**, *137*, 8038 – 8041; e) N. Ten Brummelhuis, *Polym. Chem.* **2015**, *6*, 654 – 667; f) R. M. Weiss, A. L. Short, T. Y. Meyer, *ACS Macro Lett.* **2015**, *4*, 1039 – 1043.

[5] a) R. M. Stayshich, T. Y. Meyer, *J. Am. Chem. Soc.* **2010**, *132*, 10920 – 10934; b) R. M. Weiss, E. M. Jones, D. E. Shafer, R. M. Stayshich, T. Y. Meyer, *J. Polym. Sci. Part A* **2011**, *49*, 1847 – 1855; c) J. Vandenbergh, G. Reekmans, P. Adriaensens, T. Junkers, *Chem. Commun.* **2013**, *49*, 10358 – 10360; d) J. Vandenbergh, G. Reekmans, P. Adriaensens, T. Junkers, *Chem. Sci.* **2015**, *6*, 5753 – 5761; e) J. J. Haven, J. A. De Neve, T. Junkers, *ACS Macro Lett.* **2017**, *6*, 743 – 747; f) J. Xu, C. Fu, S. Shanmugam, C. J. Hawker, G. Moad, C. Boyer, *Angew. Chem. Int. Ed.* **2017**, *56*, 8376 – 8383; *Angew. Chem.* **2017**, *129*, 8496 – 8503.

[6] a) A. Al Ouahabi, J.-A. Amalian, L. Charles, J.-F. Lutz, *Nat. Commun.* **2017**, *8*, 967; b) D. Karamessini, T. Simon-Yarza, S. Poyer, E. Konishcheva, L. Charles, D. Letourneur, J.-F. Lutz, *Angew. Chem. Int. Ed.* **2018**, *57*, 10574 – 10578; *Angew. Chem.* **2018**, *130*, 10734 – 10738; c) S. Martens, A. Landuyt, P. Espeel, B. Devreese, P. Dawyndt, F. Du Prez, *Nat. Commun.* **2018**, *9*, 4451.

[7] a) K. Lienkamp, A. E. Madkour, A. Musante, C. F. Nelson, K. Nüsslein, G. N. Tew, *J. Am. Chem. Soc.* **2008**, *130*, 9836 – 9843; b) J. Sun, X. Jiang, R. Lund, K. H. Downing, N. P. Balsara, R. N. Zuckermann, *Proc. Natl. Acad. Sci. USA* **2016**, *113*, 3954 – 3959.

[8] J. H. Swisher, J. A. Nowalk, M. A. Washington, T. Y. Meyer in *Sequence-Controlled Polymers* (Ed.: J.-F. Lutz), Wiley, Hoboken, **2017**.

[9] a) J. Hentschel, H. G. Börner, *J. Am. Chem. Soc.* **2006**, *128*, 14142 – 14149; b) S. Kessel, A. Thomas, H. G. Börner, *Angew. Chem. Int. Ed.* **2007**, *46*, 9023 – 9026; *Angew. Chem.* **2007**, *119*, 9181 – 9184; c) A. K. H. Hirsch, F. Diederich, M. Antonietti, H. G. Börner, *Soft Matter* **2010**, *6*, 88 – 91; d) G. K. Such, Y. Yan, A. P. Johnston, S. T. Gunawan, F. Caruso, *Adv. Mater.* **2015**, *27*, 2278 – 2297; e) D. Remmler, T. Schwaar, M. Pickhardt, C. Donth, E. Mandelkow, M. G. Weller, H. G. Börner, *J. Controlled Release* **2018**, *285*, 96 – 105; f) K. Sato, M. P. Hendricks, L. C. Palmer, S. I. Stupp, *Chem. Soc. Rev.* **2018**, *47*, 7539 – 7551; g) P. Wilke, N. Helfricht, A. Mark, G. Papastavrou, D. Faivre, H. G. Börner, *J. Am. Chem. Soc.* **2014**, *136*, 12667 – 12674; h) F. Hanßke, E. Kemnitz, H. G. Börner, *Small* **2015**, *11*, 4303 – 4308; i) V. Samsoninkova, B. Seidt, F. Hanßke, W. Wagermaier, H. G. Börner, *Adv. Mater. Interfaces* **2017**, *4*, 1600501; j) S. Große, P. Wilke, H. G. Börner, *Angew. Chem. Int. Ed.* **2016**, *55*, 11266 – 11270; *Angew. Chem.* **2016**, *128*, 11435 – 11440; k) J. Horsch, P. Wilke, M. Pretzler, S. Seuss, I. Melnyk, D. Remmler, A. Fery, A. Rompel, H. G. Börner, *Angew. Chem. Int. Ed.* **2018**, *57*, 15728 – 15732; *Angew. Chem.* **2018**, *130*, 15954 – 15958.

[10] a) M. von Bergen, P. Friedhoff, J. Biernat, J. Heberle, E.-M. Mandelkow, E. Mandelkow, *Proc. Natl. Acad. Sci. USA* **2000**, *97*, 5129 – 5134; b) E. F. Banwell, E. S. Abelardo, D. J. Adams, M. A. Birchall, A. Corrigan, A. M. Donald, M. Kirkland, L. C. Serpell, M. F. Butler, D. N. Woolfson, *Nat. Mater.* **2009**, *8*, 596 – 600; c) C. D. Fjell, J. A. Hiss, R. E. W. Hancock, G. Schneider, *Nat. Rev. Drug Discovery* **2012**, *11*, 37 – 51; d) B. P. Gray, K. C. Brown, *Chem. Rev.* **2014**, *114*, 1020 – 1081; e) F. Rabanal, A. Grau-Campistany, X. Vila-Farrés, J. Gonzalez-Linares, M. Borràs, J. Vila, A. Manresa, Y. Cajal, *Sci. Rep.* **2015**, *5*, 10558.

[11] S. Wieczorek, E. Krause, S. Hackbarth, B. Röder, A. K. H. Hirsch, H. G. Börner, *J. Am. Chem. Soc.* **2013**, *135*, 1711 – 1714.

[12] S. Wieczorek, A. Dallmann, Z. Kochovski, H. G. Börner, *J. Am. Chem. Soc.* **2016**, *138*, 9349 – 9352.

[13] S. Wieczorek, D. Remmler, T. Masini, Z. Kochovski, A. K. H. Hirsch, H. G. Börner, *Bioconjugate Chem.* **2017**, *28*, 760 – 767.

[14] S. Schneider, J. Marles-Wright, K. H. Sharp, M. Paoli, *Nat. Prod. Rep.* **2007**, *24*, 621 – 630.

[15] C. Hopper, A. Kübler, H. Lewis, I. B. Tan, G. Putnam, *Int. J. Cancer* **2004**, *111*, 138 – 146.

[16] R. Gref, Y. Minamitake, M. T. Peracchia, V. Trubetskoy, V. Torchilin, R. Langer, *Science* **1994**, *263*, 1600 – 1603.

Manuscript received: February 19, 2019
Accepted manuscript online: April 25, 2019
Version of record online: July 1, 2019

